Optically Active and C_3-Symmetric Tris(pyrazolyl)hydroborate and Tris(pyrazolyl)phosphine Oxide Ligands: Synthesis and Structural Characterization

Daniel D. LeCloux, Christopher J. Tokar, Masahisa Osawa, Robert P. Houser, Michael C. Keyes, and William B. Tolman*

University of Minnesota, 207 Pleasant St. S. E., Minneapolis, Minnesota 55455

Received January 20, 1994®

We report multigram-scale syntheses of optically active thallium(I) tris(pyrazolyl)hydroborate {Tl[HB(pz*)$_3$]} [pz* = 7(*R*)-isopropyl-4(*R*)-methyl-4,5,6,7-tetrahydroindazolyl (Menthpz) and 7(*S*)-*tert*-butyl-4(*R*)-methyl-4,5,6,7-tetrahydroindazolyl (Mementhpz)] and tris(pyrazolyl)-phosphine oxide [OP(pz*)$_3$] [pz* = (4*S*,7*R*)-7,8,8-trimethyl-4,5,6,7-tetrahydro-4,7-methano-2-indazolyl (Camphpz), Menthpz, and Mementhpz] ligands of potential utility for stereoselective metal-mediated organic transformations, the assignment of their ^{1}H and ^{13}C NMR spectra using COSY and HETCOR methods, and representative X-ray crystal structures that define their absolute configurations and steric properties. X-ray structure data for OP(Camphpz)$_3$: monoclinic, space group $P2_1$ (No. 4), at 24 °C, a = 6.841(4) Å, b = 18.657(8) Å, c = 12.633(4) Å, β = 103.62(4)°, V = 1567(2) Å^3, Z = 2, R = 0.052, and R_w = 0.057 for 2564 reflections with $I > 2\sigma(I)$ and 369 parameters. X-ray structure data for Tl[HB(Menthpz)$_3$] (TlTp^{Menth}): monoclinic, space group $P2_12_12_1$ (No. 19), at 24 °C, a = 9.763(3) Å, b = 18.004(7) Å, c = 20.29(2) Å, V = 3566(5) Å^3, Z = 4, R = 0.040, and R_w = 0.038 for 4497 reflections with $I > 2\sigma(I)$ and 370 parameters. X-ray structure data for Tl[HB(Mementhpz)$_3$] (TlTp^{Mementh}): monoclinic, space group $P2_12_12_1$ (No. 19), at 24 °C, a = 10.711(6) Å, b = 14.97(1) Å, c = 23.769(6) Å, V = 3811(7) Å^3, Z = 4, R = 0.050, and R_w = 0.053 for 3896 reflections with $I > 2\sigma(I)$ and 397 parameters.

Tris(pyrazolyl)hydroborate anions [Tp or HB(pz)$_3^-$] have been demonstrated to be versatile ligands useful for the preparation of complexes of elements from throughout the periodic table that are important from inorganic, organometallic, and/or bioinorganic chemistry perspectives.[1] Recent work has shown that by incorporating substituents at the pyrazolyl rings' 3-position, profound steric effects on metal complex properties such as geometry, nuclearity, spectroscopic features, and reactivity may be observed.[1,2] Many of these effects can be traced to the specific orientation of the alkyl or aryl appendages, which enclose the bound metal ion in a highly protected pocket of well-defined shape. The observed propensity of Tp ligands to strongly coordinate to a wide range of metal ions coupled with the demonstrated steric effects of pyrazolyl ring substituents suggests that chiral Tp's and derived metal complexes would be promising reagents for stereoselective metal-centered molecular recognition and/or catalysis of organic transformations. Moreover, the potential for generation of optically active ligands and complexes that have C_3 symmetry[3] offers an interesting opportunity to examine the influence on enantioselective processes of having a rotational symmetry axis higher than the more typical C_2 case.[4] Similar arguments apply to neutral variants of Tp* chelates such as OP(pz*)$_3$,[5] although the versatility of these ligands has yet to be demonstrated to the extent now known for Tp's.

In this paper we present our progress toward the construction and structural characterization of a series of novel optically active and C_3-symmetric polypyrazole ligands.[6] The multigram-scale syntheses of Tp and/or OP(pz)$_3$ ligands derived from the enantiomerically enriched pyrazoles **1**, *cis*-**2**, and *trans*-**3**, assignment of their ^{1}H and ^{13}C NMR spectra using 2D methods, and representative X-ray crystal structures that define their absolute configurations and steric properties are described. Demon-

* To whom correspondence should be addressed. FAX: 612-626-7541; E-mail: tolman@chemsun.chem.umn.edu.

® Abstract published in *Advance ACS Abstracts*, June 1, 1994.

(1) (a) Trofimenko, S. *Chem. Rev.* **1993**, *93*, 943–980. (b) Trofimenko, S. In *Progress in Inorganic Chemistry*; Lippard, S. J., Ed.; Wiley: New York, 1986; Vol. 34; pp 115–210. (c) Shaver, A. In *Comprehensive Coordination Chemistry*; Wilkinson, G., Gillard, R. D., and McCleverty, J. A., Eds.; Pergamon Press: Oxford, 1987; Vol. 2; pp 245–259. (d) Niedenzu, K.; Trofimenko, S. *Top. Curr. Chem.* **1986**, *131*, 1–37. (e) General review on the utility of nitrogen donor ligands in organometallic chemistry: Togni, A.; Venanzi, L. M. *Angew. Chem., Int. Ed. Engl.* **1994**, *33*, 497–526.

(2) Selected recent examples: (a) Long, G. J.; Grandjean, F.; Trofimenko, S. *Inorg. Chem.* **1993**, *32*, 1055–1058. (b) Rheingold, A. L.; White, C. B.; Trofimenko, S. *Inorg. Chem.* **1993**, *32*, 3471–3477. (c) Han, R.; Looney, A.; McNeill, K.; Parkin, G.; Rheingold, A. L.; Haggerty, B. S. *J. Inorg. Biochem.* **1993**, *49*, 105–121. (d) Han, R.; Parkin, G. *J. Am. Chem. Soc.* **1992**, *114*, 748–757. (e) Looney, A.; Han, R.; McNeill, K.; Parkin, G. *J. Am. Chem. Soc.* **1993**, *115*, 4690–4697. (f) Kitajima, N.; Fujisawa, K.; Tanaka, M.; Moro-oka, Y. *J. Am. Chem. Soc.* **1992**, *114*, 9232–9233. (g) Kitajima, N.; Fujisawa, K.; Fujimoto, C.; Moro-oka, Y.; Hashimoto, S.; Kitagawa, T.; Toriumi, K.; Tatsumi, K.; Nakamura, A. *J. Am. Chem. Soc.* **1992**, *114*, 1277–1291. (h) Carrier, S. M.; Ruggiero, C. E.; Houser, R. P.; Tolman, W. B. *Inorg. Chem.* **1993**, *32*, 4889–4899. (i) Ruggiero, C. E.; Carrier, S. M.; Antholine, W. E.; Whittaker, J. W.; Cramer, C. J.; Tolman, W. B. *J. Am. Chem. Soc.* **1993**, *115*, 11285–11298. (j) Looney, A.; Parkin, G. *Inorg. Chem.* **1994**, *33*, 1234–1237.

(3) (a) Adolfsson, H.; Wärnmark, K.; Moberg, C. *J. Chem. Soc., Chem. Commun.* **1992**, 1054–1055. (b) Nugent, W. A. *J. Am. Chem. Soc.* **1992**, *114*, 2768–2769. (c) Burk, M. J.; Harlow, R. L. *Angew. Chem., Int. Ed. Engl.* **1990**, *29*, 1462–1464. (d) Burk, M. J.; Feaster, J. E.; Harlow, R. L. *Tetrahedron: Asymmetry* **1991**, *2*, 569–592. (e) Ward, T. R.; Venanzi, L. M.; Albinati, A.; Lianza, F.; Gerfin, T.; Gramlich, V.; Tombo, G. M. R. *Helv. Chim. Acta* **1991**, *74*, 983–988. (f) Baker, M. J.; Pringle, P. G. *J. Chem. Soc., Chem. Commun.* **1993**, 314–316.

(4) Whitesell, J. K. *Chem. Rev.* **1989**, *89*, 1581–1590.

(5) Joshi, V. S.; Kale, V. K.; Sathe, K. M.; Sarkar, A.; Tavale, S. S.; Suresh, C. G. *Organometallics* **1991**, *10*, 2898–2902.

(6) Aspects of this work have been communicated: (a) Tokar, C. J.; Kettler, P. B.; Tolman, W. B. *Organometallics* **1992**, *11*, 2738–2739. (b) LeCloux, D. D.; Tolman, W. B. *J. Am. Chem. Soc.* **1993**, *115*, 1153–1154.

0276-7333/94/2313-2855$04.50/0 © 1994 American Chemical Society

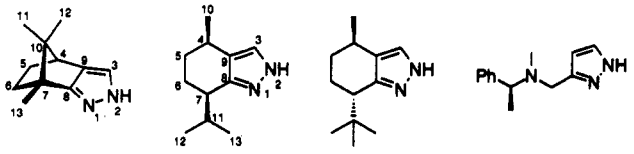

1 *cis*-2 *trans*-3 4

stration of wide-ranging metal binding properties of the new Tp* ligands will appear in a separate paper.[7]

A procedure for the synthesis of 1 has appeared, but we have modified the reaction conditions and workup slightly in order to access it in higher yield.[8] Pyrazole 2 has also been reported by a route similar to the one we have used, but it was not isolated in enantiomerically enriched form.[9] Approaches to optically active pyrazoles different from that which we report (*vide infra*) have appeared in the recent literature;[8a,10] included among them is a versatile method involving condensation of an optically active amine with an acylpyrazole to give an amide, which is then reduced to an optically active pyrazole (e.g., 4).[8a]

Although mixtures of regioisomers were observed in published attempts to N-alkylate 1 (bond formation at N1 and N2),[11] it was used to build a tetra(pyrazolyl)borate ligand linked exclusively at N2 which formed a complex with copper(I) that catalyzed the enantioselective cyclopropanation of styrene with ethyl diazoacetate.[12] Subsequent to our preliminary publication of its enantioselective synthesis,[6b] elaboration of *cis*-2 into a bis(pyrazolyl)methane ligand that was used in Pd-catalyzed asymmetric allylic alkylation reactions was noted.[13] A Tp* ligand constructed from 4 was identified on the basis of mass spectrometric and ^{1}H NMR and IR spectroscopic measurements.[8b]

Results and Discussion

Synthetic Strategy. In principle, there are at least two ways to construct optically active Tp or OP(pz)$_3$ ligands. Three different pyrazoles could be attached to a single B atom or O=P unit to form a tetrahedral and stereogenic B or P center, respectively, or three identical, yet already chiral, pyrazoles could be linked to yield a C_3-symmetric ligand. The first route is particularly daunting experimentally for the following reasons. First, in a Tp synthesis intermolecular pyrazole exchange is facile under the usual thermolytic conditions employed in order to eliminate H_2 and forge the B–N bonds from the starting pyrazole(s) and MBH_4 (M = Na or K); thus, a statistical mixture of isomers $[HB(pz)_3]^-$, $[HB(pz)_2(pz')]^-$, $[HB(pz)(pz')(pz'')]^-$, etc. would be expected. Second, even if chiral $[HB(pz)(pz')(pz'')]^-$ or OP(pz)(pz')(pz'') isomers could be isolated, each would have to be resolved in order to access the enantiomerically pure forms. The syntheses of the unsymmetrical bis(pyrazolyl)hydroborates $[H_2B(pz)(3,5\text{-dimethylpz})]^-$[14] and $[H_2B(3\text{-}CF_3\text{-}5\text{-}CH_3pz)(3\text{-}CH_3\text{-}5\text{-}CF_3pz)]^-$[15] comprise some progress toward ligands with stereogenic boron atoms, but no reports of their elaboration to such molecules have published.

We have thus focused on the second method, which involves the assembly of three identical enantiomerically pure pyrazoles (Hpz*) into Tp* or OP(pz*)$_3$ ligands. Annulated pyrazoles 1–3 were targeted because the critical stereogenic center attached to the pyrazole carbon α to the free N (the N atom not linked to the B or P centers in the targeted ligands) would be held in a relatively rigid conformation and because their synthesis could be envisioned starting from inexpensive and readily available precursors (1*R*)-(+)-camphor, (2*S*,5*R*)-(−)-menthone, and a (*R*)-(+)-pulegone, respectively. On the basis of the known preference for B–N bond formation during Tp syntheses to occur at the least hindered nitrogen atoms of substituted pyrazoles,[16] the critical conformationally restricted stereogenic carbon was anticipated to reside exclusively in the desired position distal to the central B or P linker and proximate to a coordinated metal center:

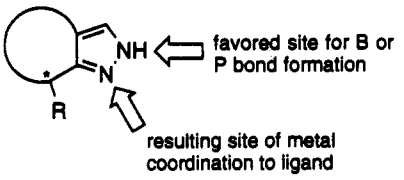

Ligand Synthesis. (a) Pyrazoles. The syntheses of 1, *cis*-2, and *cis*- and *trans*-3 are outlined in Scheme 1; all involve formylation at the less hindered α position of a ketone followed by cyclocondensation of the resulting hydroxymethylene-carbonyl compound with hydrazine via well-established methods.[17] The procedure we have developed for the preparation of 1 is more straightforward than that reported previously[8a,18] and affords the product in higher yield [84% overall from (1*R*)-(+)-camphor] on a >8-g scale. In the synthesis of *cis*-2, epimerization of the carbon atom α to the carbonyl occurred during formylation of (2*S*,5*R*)-menthone to give a 13:1 ratio of diastereomeric (3*R*,6*R*)- and (3*R*,6*S*)-2-(hydroxymethylene)-6-isopropyl-3-methylcyclohexanones [(3*R*,6*R*)- and (3*R*,6*S*)-5] after purification by chromatography and distillation. Separation of these diastereomers proved to be problematic, so the mixture was treated with 1 equiv of hydrazine monohydrate to yield pyrazoles *cis*- and *trans*-2 in the same 13:1 ratio. In a preliminary report, separation of the pyrazole diastereomers was accomplished by fractional crystallization of their bisulfate salts.[6b] We have since found that large-scale (35 g) fractional crystallization of the hydrochloride salts is more readily accomplished, yielding (after conversion of the purified salt to the free base) the major diastereomer *cis*-2 in 20% overall yield [from (2*S*,5*R*)-menthone] >95% pure by ^{1}H NMR spectroscopy (other isomer not observed).

(7) LeCloux, D. D.; Osawa, M.; Reynolds, V.; Keyes, M. C.; Tolman, W. B. To be submitted for publication.
(8) (a) Brunner, H.; Scheck, T. *Chem. Ber.* **1992**, *125*, 701–709. (b) Scheck, T. Ph.D. Thesis, Universität Regensburg, 1991.
(9) Elguero, J.; Shimizu, B. *An. Quim.* **1988**, *84*, 183–190.
(10) Kashima, C.; Fukuchi, I.; Takahashi, K.; Hosomi, A. *Tetrahedron Lett.* **1993**, *34*, 8305–8308.
(11) (a) Watson, A. A.; House, D. A.; Steel, P. J. *J. Org. Chem.* **1991**, *56*, 4072–4074. (b) Watson, A. A.; House, D. A.; Steel, P. J. *Inorg. Chim. Acta* **1987**, *130*, 167–176. (c) House, D. A.; Steel, P. J.; Watson, A. A. *Aust. J. Chem.* **1986**, *39*, 1525–1536.
(12) Brunner, H.; Singh, U. P.; Boeck, T.; Altmann, S.; Scheck, T.; Wrackmeyer, B. *J. Organomet. Chem.* **1993**, *443*, C16–C18.
(13) Bovens, M.; Togni, A.; Venanzi, L. M. *J. Organomet. Chem.* **1993**, *451*, C28–C31.
(14) Frauendorfer, E.; Agrifoglio, G. *Inorg. Chem.* **1982**, *21*, 4122–4125.
(15) Krentz, R. Ph.D. Thesis, University of Alberta, 1989.
(16) For examples, see: (a) Trofimenko, S.; Calabrese, J. C.; Thompson, J. S. *Inorg. Chem.* **1987**, *26*, 1507–1514. (b) Trofimenko, S.; Calabrese, J. C.; Domaille, P. J.; Thompson, J. S. *Inorg. Chem.* **1989**, *28*, 1091–1101. (c) Calabrese, J. C.; Trofimenko, S. *Inorg. Chem.* **1992**, *31*, 4810–4814.
(17) (a) Fusco, R. In *Pyrazoles, Pyrazolines, Pyrazolidines, Indazoles, and Condensed Rings*; Wiley, R. H., Ed.; Interscience: New York, 1967; pp 1–176. (b) Potts, K. T. *Comprehensive Heterocyclic Chemistry*; Pergamon: Oxford, 1984; Vol. 5.
(18) Jacquier, R.; Maury, G. *Bull. Soc. Chim. Fr.* **1967**, 295–297.

Scheme 1

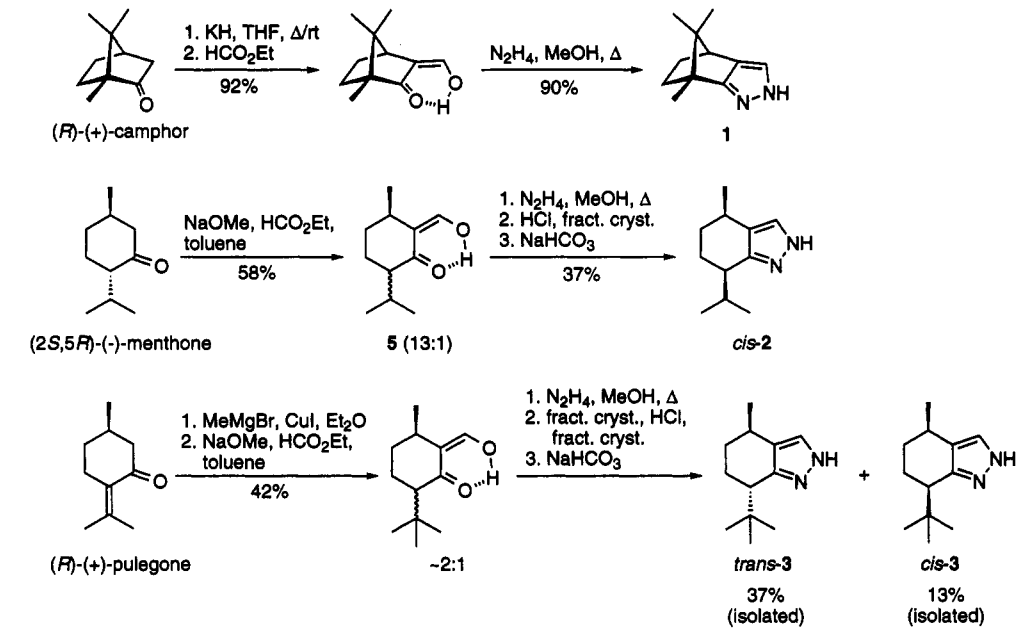

Scheme 2

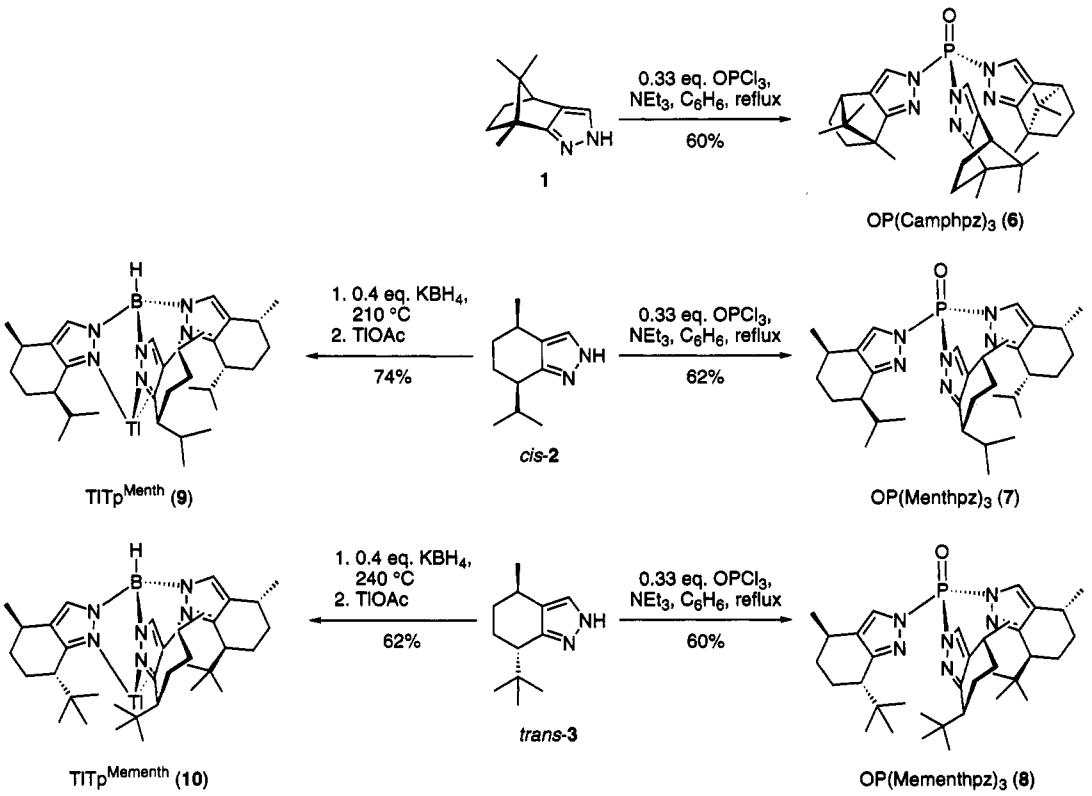

The synthesis of **3** proceeded similarly to that of *cis*-**2**, except the 2-*tert*-butyl-5(*R*)-methylcyclohexanone precursor had to be prepared from (*R*)-(+)-pulegone, a task which we accomplished via methylcuprate addition based on a published procedure.[19,20] In addition, the diastereomeric pyrazoles *cis*- and *trans*-**3** were obtained in a ~2:1 instead of a 13:1 ratio. Thus, in contrast to the case of **2** where only one (major) isomer could be isolated, the diastereomers of **3** were separately isolated >95% pure, in 5% and 15% yield, respectively [based on (*R*)-(+)-pulegone], via a protocol involving a combination of direct crystallizations and fractional crystallizations of the hydrochloride salts (see Experimental Section for details).

(b) Ligands. A set of new optically active and C_3-symmetric OP(pz*)$_3$ and TlTp* ligands was prepared in good yields from **1**, *cis*-**2**, and *trans*-**3** by procedures analogous to those reported previously for achiral variants (Scheme 2).[1,5] Thus, the phosphine oxides **6–8** were constructed by substitution of the chlorides of $OPCl_3$ by the appropriate pyrazoles in the presence of triethylamine in refluxing benzene, while the TlTp* ligands **9** and **10** were prepared by thermolysis of the pyrazoles with KBH_4. Attempts to isolate a Tp* from **1** or either type of ligand

(19) Djerassi, C.; Hart, P. A.; Warawa, E. J. *J. Am. Chem. Soc.* **1964**, *86*, 78–85.
(20) Corey, E. J.; Ensley, H. E. *J. Am. Chem. Soc.* **1975**, *97*, 6908–6909.

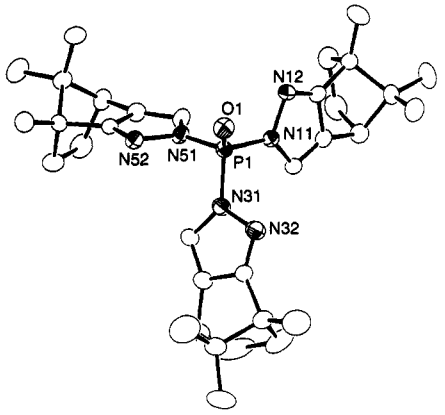

Figure 1. ORTEP representation of the X-ray crystal structure of OP(Camphpz)$_3$ (**6**), with atom labels for all non-carbon atoms (35% ellipsoids, H atoms omitted for clarity). Selected bond lengths (Å) and bond angles (deg): P1–O1, 1.448(3); P1–N11, 1.667(4); P1-N31, 1.672(4); P1-N51, 1.673-(4); O1-P1-N11, 115.4(2); O1-P1-N31, 114.5(2); O1–P1–N51, 116.8(2); N11–P1–N31, 103.1(2); N11–P1–N51, 102.1(2); N31–P1–N51, 103.0(2).

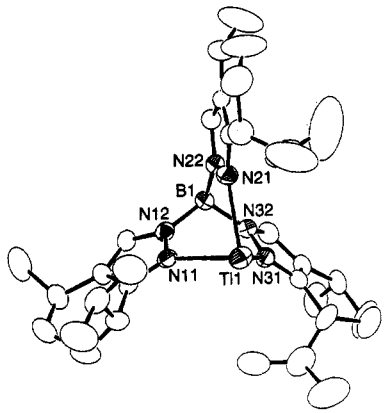

Figure 2. ORTEP representation of the X-ray crystal structure of TlTp^{Menth} (**9**), with atom labels for all non-carbon atoms (35% ellipsoids, H atoms omitted for clarity). Selected bond lengths (Å) and bond angles (deg): Tl1–N11, 2.530(7); Tl1–N21, 2.574(7); Tl1–N31, 2.546(7); N11–Tl1–N21, 72.7-(2); N11–Tl1–N31, 79.0(2); N21–Tl1–N31, 75.2(2).

from *cis*-**3** failed, however. In the former case, NMR spectroscopic analysis of the crude product indicated formation of a mixture after heating of **1** in the presence of KBH_4 under a variety of different conditions, suggesting either poor regioselectivity in the B–N bond-forming reaction or generation of mono-, bis-, tris-, and/or tetra-(pyrazolyl)borates. The inability of *cis*-**3** to assemble into tridentate ligands is difficult to rationalize; prohibitive steric effects apparently arise from conformational preferences in this diastereomer that differ in some way from those in the analogous, albeit presumabley less hindered, *cis*-**2**.

The synthesis of Tp^{Menth} [the Tp* derived from *cis*-**2**] is much improved from the previously reported method, which involved sequential thermolysis of *cis*-**2** and KBH_4 in DMAC and anisole solutions to give the potassium salt of the ligand contaminated with unreacted pyrazole.[6b] This crude product had to be used directly for metal complex synthesis because attempts to generate the more crystalline thallium complex using aqueous $TlNO_3$ according to published procedures[16] resulted in substantial ligand decomposition (regeneration of pyrazole by hydrolytic B–N bond cleavage). A more straightforward procedure which circumvented this problem and afforded superior yields of crystalline TlTp^{Menth} (**9**) and TlTp^{Mementh} (**10**) involved slow heating of the pyrazoles and KBH_4 to the indicated temperature with monitoring of H_2 evolution, followed by treatment with a slurry of TlOAc in CH_2Cl_2 (Scheme 2).

Table 1. Crystallographic Data for OP(Camphpz)$_3$ (6), TlTp^{Menth} (9), and TlTp^{Mementh} (10)

	6	**9**	**10**
formula	$C_{33}H_{45}N_6OP$	$C_{33}H_{52}N_6BTl$	$C_{36}H_{58}N_6BTl$
formula wt (g mol^{-1})	572.73	747.99	790.07
space grp	$P2_1$ (#4)	$P2_12_12_1$ (#19)	$P2_12_12_1$ (#19)
a (Å)	6.841(4)	9.763(3)	10.711(6)
b (Å)	18.657(8)	18.004(7)	14.97(1)
c (Å)	12.633(4)	20.29(2)	23.769(6)
β (deg)	103.62(4)		
V (Å^3)	1567(2)	3566(5)	3811(7)
Z	2	4	4
ρ_{calcd} (g cm^{-1})	1.214	1.393	1.377
μ (cm^{-1})	1.18	46.00	43.09
temp (°C)	24	24	24
radiation, λ (Å)	Mo Kα, 0.710 69	Mo Kα, 0.710 69	Mo Kα, 0.710 69
$2\theta_{max}$ (deg)	53.9	48.0	56.0
total no. of data collected	7032	5970	7394
total no. of unique data[a]	3528	3185	7134
total no. unique data with $I > 2\sigma(I)$	2564	4497	3896
no. of variable param	369	370	397
R^b	0.052	0.040	0.050
$R_w{}^b$	0.057	0.038	0.053

[a] R_{int} values: 0.056 (**6**); 0.111 (**9**); 0.038 (**10**). [b] $R = \Sigma||F_o|-|F_c||/\Sigma|F_o|$; $R_w = [(\Sigma w(|F_o|-|F_c|)^2/\Sigma wF_o^2)]^{1/2}$, where $w = 4F_o^2/s^2(F_o^2)$ and $s^2(F_o^2) = [S^2(C + R^2B) + (pF_o^2)^2]/L_p^2$ with S = scan rate, C = total integrated peak count, R = ratio of scan time to background counting time, B = total background count, L_p = Lorentz polarization factor, and $p = p$-factor (0.03 for **9** and 0.05 for **6** and **10**).

X-ray Crystal Structures. ORTEP representations and stereoviews of the X-ray crystal structures of OP-(Camphpz)$_3$ (**6**), TlTp^{Menth} (**9**), and TlTp^{Mementh} (**10**) are shown in Figures 1–5. Crystallographic data are summarized in Table 1, and selected positional parameters are listed in Tables 2–4. The P–O and P–N_{pz} bond lengths in **6** [1.448(3) Å and 1.67 Å (avg), respectively] are similar to those reported in the literature for analogous P=O and P–$N_{heterocycle}$ bonds.[5,21] The structural parameters of the camphpz groups are closely analogous to those reported previously for ligands and complexes containing this unit.[9bc,22] The most noteworthy facet of the structure of **6** (Figure 1) is the observed P–N bond formation exclusively at N2. Similar regiospecificity was postulated on the basis of spectroscopic data for Na[B(pz*)$_4$] (Hpz* = 1),[8b,10] but N-alkylations of **1** were reported to give mixtures of N1- and N2-linked regioisomers.[9]

The X-ray structures of **9** and **10** (Figures 2/3 and 4/5, respectively) reveal tridentate binding of the tris(pyrazolyl)hydroborate ligands to Tl(I) and conclusively evince the absolute configurations of the pyrazolyl components. Similar to the majority of other reported examples of Tl-(I) complexes of achiral Tp ligands,[23] both **9** and **10** are monomeric, show linkage of the most hindered N_{pz} atoms to the Tl atom, and exhibit average Tl–N bond lengths that fall within the relatively narrow range 2.50–2.60 Å.

(21) Allen, F. H.; Kennard, O.; Watson, D. G.; Brammer, L.; Orpen, A. G.; Taylor, R. *J. Chem. Soc., Perkin Trans. I* **1987**, S1–S19.

(22) (a) Steel, P. J. *Acta Crystallogr.* **1983**, *C39*, 1623–1625. (b) House, D. A.; Steel, P. J.; Watson, A. A. *J. Chem. Soc., Chem. Commun.* **1987**, 1575–1576. (c) Watson, A. A.; House, D. A.; Steel, P. J. *Polyhedron* **1989**, *8*, 1345–1350.

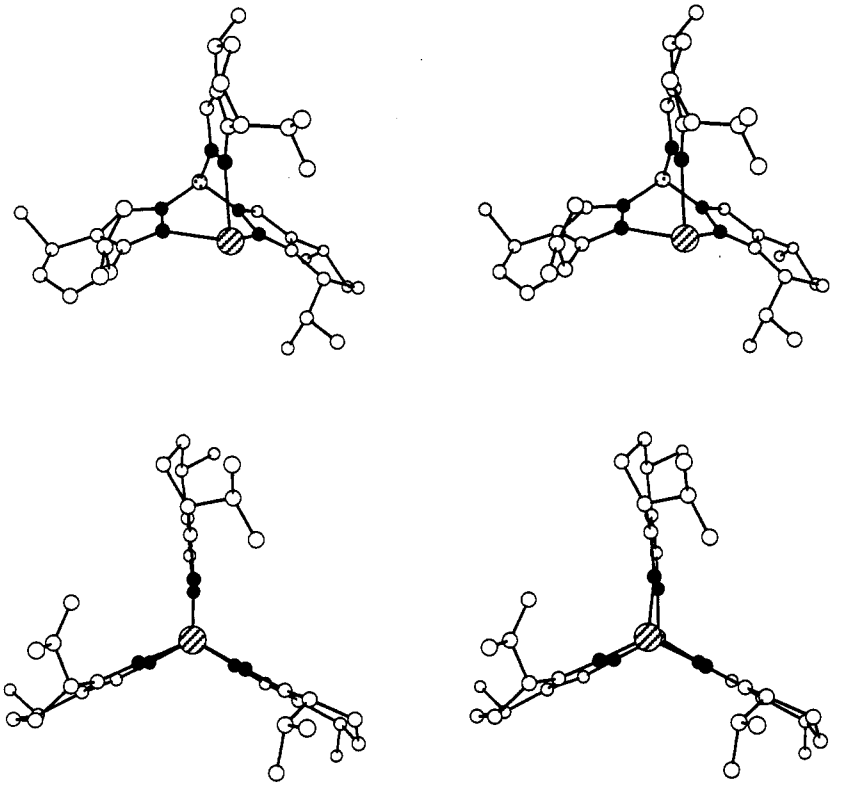

Figure 3. Stereoviews of the X-ray crystal structure of TlTp^{Menth} (**9**), with perspectives similar to the ORTEP drawing (top) and down the Tl···B–H vector (bottom).

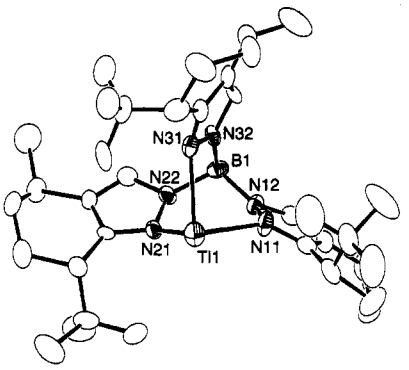

Figure 4. ORTEP representation of the X-ray crystal structure of TlTp^{Mementh} (**10**), with atom labels for all non-carbon atoms (35% ellipsoids, H atoms omitted for clarity). Selected bond lengths (Å) and bond angles (deg): Tl1–N11, 2.56(1); Tl1–N21, 2.520(9); Tl1–N31, 2.589(9); N11–Tl1–N21, 79.1(3); N11–Tl1–N31, 77.5(4); N21–Tl1–N31, 74.2(4).

It has been suggested[23c] that these values indicate that the bonding between Tl and the N donor atoms of the Tp ligands is composed of a combination of normal covalent and dative covalent interactions because the bond distances are greater than the sum of the covalent radii of Tl (1.57 Å) and N (0.74 Å).[24] The 4-carbon (containing the methyl group) has an *R* configuration in both ligands, but in **9** (and in the diastereomer of **2** from which **9** is derived) the 7-isopropyl substituent is *cis* to the 4-methyl (*R* configuration), while in **10** (and in the diastereomer of **3** from which **10** is derived) the 7-*tert*-butyl group is in a *trans* position (*S* configuration). The resulting approximately C_3-symmetric array of sterically bulky substituents on the stereogenic centers surrounding the Tl(I) ion in **9** thus has opposite rotational stereochemistry compared to that of **10** (C7 substituents point clockwise vs counterclockwise, respectively), an aspect that is most readily apparent in the views along the Tl···B–H vectors in the bottoms of Figures 3 and 5.

In addition to their contrasting relative rotational stereochemistries, significant differences in the geometric features of the two Tp* ligands arise as a result of the divergent steric properties of the 7-substituents. The local symmetry about the Tl(I) ion in **9** (not including the chiral 6-membered rings annulated to the pyrazoles) is only slightly distorted from C_{3v}, as indicated by the dihedral angles between the pyrazolyl ring planes (127.3°, 123.9°, and 108.7°) and the torsion angles Tl1–N11–N12–C13, Tl1–N21–N22–C23, and Tl1–N31–N32–C33 that are close to 180° [175.5(5)°, 173.5(5)°, and 177.8(6)°, respectively]. In contrast, the analogous torsion angles in **10** are 159.5(7)°, 139.9(9)°, and 142.4(9)°, values which significantly deviate from 180° and thus reflect the severe "propellor-like" distortion of the array of pyrazolyl rings in this ligand. This distortion, which to our knowledge has not been seen previously in any other crystal structures of Tp complexes, probably arises from unfavorable intramolecular nonbonding interactions involving the 7-*tert*-butyl groups that are greater than those involving alternative substituents in other ligands. As a result, the Tl–N_{pz} bond vectors in **10** are not coincident with the expected vectors comprised of the lone pair of electrons donated by each pyrazolyl nitrogen atom to the Tl center; presumably, this lack of directionality in the bonding interactions reflects a degree of noncovalency or ionic character in the system.

NMR Properties. A detailed study of the NMR properties of the new optically active polypyrazole ligands

(23) (a) Cowley, A. H.; Geerts, R. L.; Nunn, C. M.; Trofimenko, S. *J. Organomet. Chem.* **1989**, *365*, 19–22. (b) Ferguson, G.; Jennings, M. C.; Lalor, F. J.; Shanahan, C. *Acta Crystallogr.* **1991**, *C47*, 2079–2082. (c) Libertini, E.; Yoon, K.; Parkin, G. *Polyhedron* **1993**, 2539–2542. (d) Parkin, G. Unpublished results.

(24) Haaland, A. *Angew. Chem., Int. Ed. Engl.* **1989**, *28*, 992–1007.

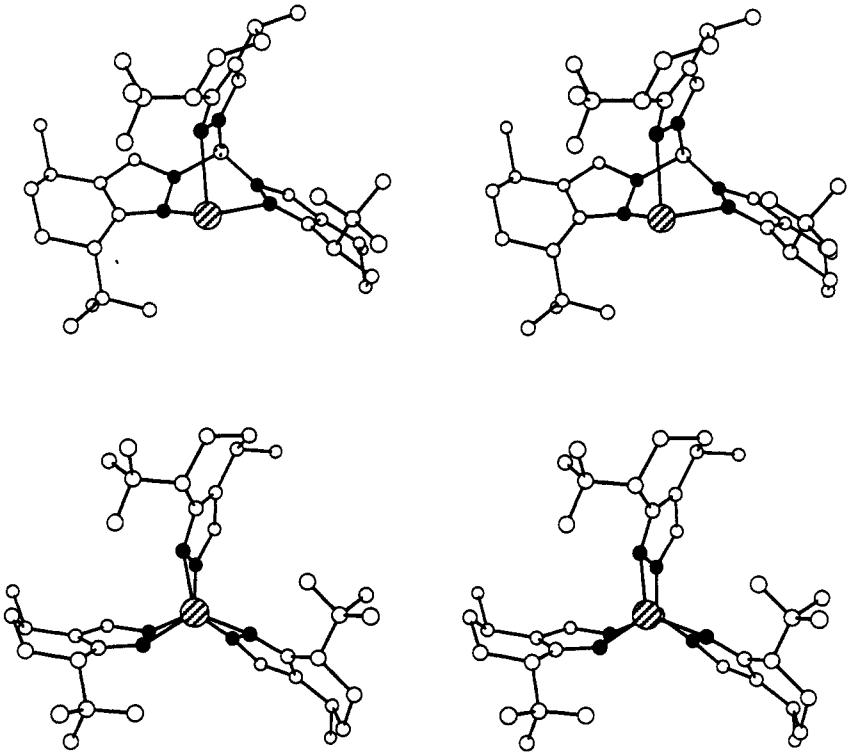

Figure 5. Stereoviews of the X-ray crystal structure of $TlTp^{Mementh}$ (**10**), with perspectives similar to the ORTEP drawing (top) and down the Tl···B–H vector (bottom).

was undertaken in an attempt to correlate the structures determined in the solid state with those adopted in solution. ^1H and $^{13}C\{^1H\}$ NMR spectroscopic data and proposed assignments based on ^1H–^1H COSY and ^1H–^{13}C HETCOR experiments for pyrazoles *cis*-**2**, *cis*- and *trans*-**3**, and ligands **6**–**10** are listed in Table 5. The 2D spectra are supplied as supplementary material. The data for the pyrazoles, in particular the ^{13}C chemical shifts, agree well with published results for achiral, substituted pyrazoles.[25] Unfortunately, corroboration by NMR spectroscopy of the absolute configurations assigned by X-ray crystallography for the pyrazoles and derived ligands has not been possible so far due to our inability (even with NOESY data) to conclusively attribute resonances to specific methylene hydrogens in the aliphatic rings (e.g., hydrogens 5a vs 5b, 6a vs 6b).

Noteworthy NMR spectroscopic features of the phosphine oxide ligands include large downfield shifts of the C8 ^{13}C resonance compared to that in the respective free pyrazole ($\Delta\delta > 10$ ppm) and discernable coupling between the pyrazole ring carbons and the phosphorus atom. The regioselectivity of P–N bond formation was identified for **6** from ^1H–^{31}P NOE difference spectroscopy (we assign similar connectivity in **7** and **8** by analogy). Specifically, irradiation of H3 in **6** induced significantly greater enhancement of the ^{31}P resonance (32%) than irradiation of H13 (23%), consistent with the closer proximity of H3 to the phosphorus atom and attachment to N2 as proven by the X-ray structure.

An interesting and potentially informative property of the Tl(I) complexes **9** and **10** is the presence of ^{205}Tl ($I = {}^1/_2$) coupling in their ^{13}C NMR spectra and related broadening of ^1H NMR signals (Table 5). Analogous phenomena have been reported for other Tl(I) complexes

(25) Lopez, C.; Claramunt, R. M.; Trofimenko, S.; Elguero, J. *Can. J. Chem.* **1993**, *71*, 678–684.

Table 2. Selected Positional Parameters for $OP(Camphpz)_3$ (6)

atom	*x*	*y*	*z*	*B*(eq) (Å²)
P1	0.7540(2)	0.1831(1)	0.98965(9)	2.71(4)
O1	0.9310(5)	0.1380(2)	1.0182(3)	3.9(1)
N11	0.6725(6)	0.2155(2)	1.0945(3)	2.9(2)
N12	0.6530(7)	0.1675(2)	1.1769(3)	3.2(2)
N31	0.7824(6)	0.2567(2)	0.9193(3)	3.4(2)
N32	0.9396(7)	0.3036(3)	0.9656(3)	4.6(2)
N51	0.5456(6)	0.1458(2)	0.9133(3)	2.9(1)
N52	0.5589(6)	0.1131(2)	0.8152(3)	2.9(1)
C13	0.5560(7)	0.2049(2)	1.2345(4)	2.9(2)
C14	0.5086(7)	0.2750(3)	1.1959(4)	3.0(2)
C15	0.5825(7)	0.2809(2)	1.1057(4)	2.9(2)
C16	0.4726(8)	0.1946(3)	1.3331(4)	3.3(2)
C17	0.2390(9)	0.1938(4)	1.2879(4)	4.7(2)
C18	0.1891(8)	0.2715(4)	1.2466(5)	4.8(3)
C19	0.3952(8)	0.3085(3)	1.2704(4)	3.6(2)
C20	0.5016(8)	0.2728(3)	1.3810(4)	3.5(2)
C21	0.558(1)	0.1331(4)	1.4070(5)	5.6(3)
C22	0.7265(9)	0.2930(3)	1.4177(5)	4.7(3)
C23	0.402(1)	0.2872(4)	1.4738(4)	5.5(3)
C33	0.9271(8)	0.3534(3)	0.8933(4)	3.3(2)
C34	0.7708(8)	0.3428(3)	0.7994(4)	3.8(2)
C35	0.6798(7)	0.2819(3)	0.8183(4)	3.5(2)
C36	1.0316(9)	0.4223(3)	0.8813(4)	4.3(2)
C37	0.869(1)	0.4801(3)	0.8870(7)	7.0(4)
C38	0.703(1)	0.4689(4)	0.7843(9)	8.1(4)
C39	0.777(1)	0.4066(3)	0.7289(5)	5.3(3)
C40	1.010(1)	0.4206(3)	0.7559(5)	4.5(2)
C41	1.240(1)	0.4358(4)	0.9515(6)	8.0(4)
C42	1.070(1)	0.4907(4)	0.7091(6)	6.9(4)
C43	1.126(2)	0.3610(5)	0.7161(8)	8.4(5)
C53	0.3723(7)	0.0912(2)	0.7760(4)	2.5(2)
C54	0.2398(7)	0.1064(3)	0.8421(4)	3.0(2)
C55	0.3484(7)	0.1426(3)	0.9287(4)	3.0(2)
C56	0.2574(7)	0.0546(2)	0.6738(3)	2.7(2)
C57	0.1210(8)	0.1161(3)	0.6137(4)	4.1(2)
C58	−0.0288(8)	0.1309(3)	0.6851(5)	4.5(2)
C59	0.0383(7)	0.0791(3)	0.7818(4)	3.4(2)
C60	0.1046(7)	0.0128(3)	0.7254(4)	3.2(2)
C61	0.3751(8)	0.0133(3)	0.6080(4)	3.8(2)
C62	0.2006(9)	−0.0454(3)	0.8042(5)	4.2(2)
C63	−0.0664(8)	−0.0223(3)	0.6400(5)	4.7(2)

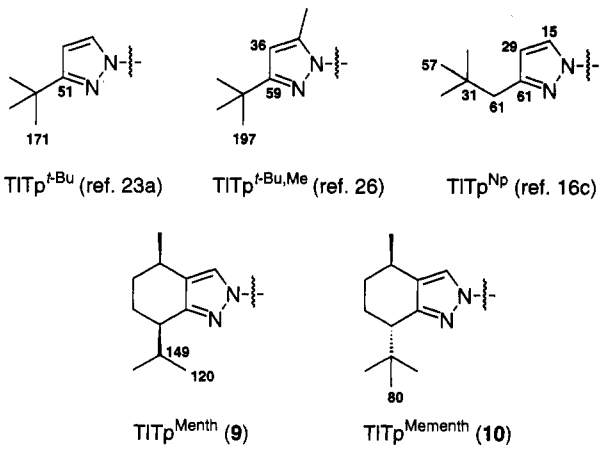

Figure 6. Observed $^{205}Tl-^{13}C$ coupling constants (Hz) for TlTp ligands. Only one pyrazolyl ring from each ligand is shown.

Table 3. Selected Positional Parameters for TlTp^{Menth} (9)

atom	x	y	z	B(eq) (Å²)
Tl1	-0.01144(3)	0.05090(2)	0.01075(2)	5.04(1)
N11	0.2095(7)	0.0262(4)	0.0721(3)	4.1(4)
N12	0.3302(7)	0.0157(4)	0.0402(3)	4.1(4)
N21	0.1025(6)	-0.0625(4)	-0.0437(3)	4.0(3)
N22	0.2407(6)	-0.0613(4)	-0.0541(3)	3.8(3)
N31	0.1631(7)	0.1056(4)	-0.0689(4)	4.6(4)
N32	0.2892(7)	0.0760(4)	-0.0724(3)	4.2(4)
C13	0.4324(9)	0.0093(5)	0.0839(4)	4.6(4)
C14	0.379(1)	0.0171(5)	0.1470(4)	4.5(5)
C15	0.242(1)	0.0272(4)	0.1366(4)	4.1(4)
C16	0.135(1)	0.0335(6)	0.1903(4)	6.1(6)
C17	0.211(1)	0.057(1)	0.2517(5)	9.3(8)
C18	0.338(1)	0.0258(9)	0.2650(5)	9.4(9)
C19	0.448(1)	0.0182(5)	0.2134(4)	5.3(5)
C23	0.2807(9)	-0.1278(5)	-0.0761(4)	3.9(4)
C24	0.166(1)	-0.1740(5)	-0.0807(5)	4.2(5)
C25	0.0580(8)	-0.1309(6)	-0.0602(4)	3.9(4)
C26	-0.089(1)	-0.1579(6)	-0.0550(5)	5.1(6)
C27	-0.077(1)	-0.2423(7)	-0.0479(6)	7.1(7)
C28	0.009(1)	-0.2783(5)	-0.1009(5)	7.8(6)
C29	0.160(1)	-0.2541(6)	-0.1008(6)	5.6(6)
C33	0.368(1)	0.1135(5)	-0.1152(4)	4.8(5)
C34	0.293(1)	0.1710(5)	-0.1409(4)	5.2(5)
C35	0.167(1)	0.1630(5)	-0.1121(4)	4.9(5)
C36	0.040(1)	0.2097(6)	-0.1249(6)	7.1(7)
C37	0.078(2)	0.2647(8)	-0.1812(7)	10(1)
C38	0.219(2)	0.287(1)	-0.1899(8)	13(1)
C39	0.325(1)	0.2293(6)	-0.1902(5)	7.1(7)
C101	0.049(1)	-0.035(1)	0.2000(7)	11(1)
C102	0.032(2)	-0.0881(9)	0.1516(7)	13(1)
C103	-0.069(1)	-0.017(1)	0.2438(8)	13(1)
C104	0.535(1)	-0.0510(7)	0.2255(5)	8.4(7)
C201	-0.178(1)	-0.1326(8)	-0.1128(5)	6.5(6)
C202	-0.192(1)	-0.0496(9)	-0.1173(6)	9.0(8)
C203	-0.318(1)	-0.1682(9)	-0.1133(7)	10(1)
C204	0.226(1)	-0.2698(7)	-0.1656(8)	9.4(9)
C301	-0.024(2)	0.2455(8)	-0.0659(8)	11(1)
C302	0.073(2)	0.305(1)	-0.037(1)	21(2)
C303	-0.159(2)	0.282(1)	-0.077(1)	17(2)
C304	0.462(2)	0.2602(9)	-0.1828(9)	15(1)
B1	0.333(1)	0.0043(6)	-0.0343(5)	4.1(5)

of sterically hindered Tp ligands (Figure 6).[16c,23a,b,26] Because the largest effects are seen in the peaks arising from the pyrazolyl substituents that lie in closest proximity to the complexed Tl(I) ion in most of the previously reported instances, it has been suggested that the involved nuclear interactions have a predominantly through-space, rather than through-bond, component.[16c,23ab,26] However, consideration of our results and the extant literature on ^{13}C coupling to Tl(I) and Tl(III) ions suggests that interpretation of the NMR results is less straightforward.

Table 4. Selected Positional Parameters for TlTp^{Mementh} (10)

atom	x	y	z	B(eq) (Å²)
Tl1	0.25070(8)	0.23185(3)	0.22587(2)	4.66(2)
N11	0.433(1)	0.2849(8)	0.2873(4)	4.4(6)
N12	0.518(1)	0.3335(7)	0.2604(4)	3.3(5)
N21	0.415(1)	0.2609(7)	0.1522(4)	3.2(5)
N22	0.479(1)	0.3394(8)	0.1560(4)	4.2(6)
N31	0.250(2)	0.4028(6)	0.2095(3)	4.4(5)
N32	0.368(1)	0.4417(8)	0.2195(5)	3.2(6)
C13	0.626(1)	0.3301(8)	0.2919(5)	3.8(7)
C14	0.613(1)	0.280(1)	0.3384(5)	4.1(7)
C15	0.486(2)	0.2530(8)	0.3339(5)	6(1)
C16	0.412(2)	0.194(1)	0.3773(6)	6(1)
C17	0.512(3)	0.153(1)	0.419(1)	10(1)
C18	0.644(3)	0.149(1)	0.3987(8)	10(1)
C19	0.687(2)	0.244(2)	0.3818(9)	8(1)
C20	0.312(2)	0.242(1)	0.4086(7)	8(1)
C23	0.496(1)	0.3747(8)	0.1017(6)	3.8(7)
C24	0.447(1)	0.3194(8)	0.0642(5)	3.6(6)
C25	0.395(1)	0.2478(6)	0.0964(5)	2.8(6)
C26	0.324(1)	0.1690(9)	0.0754(5)	4.6(7)
C27	0.297(1)	0.186(1)	0.0095(6)	5.4(8)
C28	0.294(1)	0.283(1)	-0.0086(5)	6(1)
C29	0.418(2)	0.330(1)	0.0021(5)	5.8(9)
C30	0.388(2)	0.0759(9)	0.0838(7)	6(1)
C33	0.345(1)	0.521(1)	0.2439(5)	3.7(7)
C34	0.218(1)	0.536(1)	0.2510(5)	3.5(7)
C35	0.167(1)	0.461(1)	0.2289(6)	3.3(7)
C36	0.032(2)	0.441(1)	0.2182(7)	5.2(9)
C37	-0.046(1)	0.514(1)	0.2525(7)	7(1)
C38	0.028(2)	0.559(1)	0.3022(6)	7(1)
C39	0.149(1)	0.604(1)	0.2800(6)	4.8(7)
C40	-0.014(1)	0.431(1)	0.1576(5)	4.5(8)
C101	0.826(3)	0.250(2)	0.373(1)	15(2)
C102	0.236(3)	0.182(1)	0.4524(7)	11(1)
C103	0.212(2)	0.272(2)	0.372(1)	11(2)
C104	0.363(3)	0.327(1)	0.4393(9)	13(2)
C201	0.410(2)	0.428(1)	-0.0143(7)	9(1)
C202	0.386(2)	0.054(1)	0.1462(7)	6(1)
C203	0.295(4)	0.004(1)	0.0551(9)	16(2)
C204	0.521(1)	0.079(1)	0.0578(8)	7(1)
C301	0.235(3)	0.648(1)	0.3260(7)	11(1)
C302	0.024(1)	0.510(1)	0.1243(6)	7(1)
C303	-0.157(2)	0.421(1)	0.1580(7)	8(1)
C304	0.033(1)	0.346(1)	0.1335(7)	5(1)
B1	0.494(1)	0.395(1)	0.2128(7)	3.5(8)

Through-bond coupling constants to thallium have generally been found to be quite large, and they vary in rather unpredictable ways with the number of intervening bonds, the hybridization of the atoms involved, and other factors.[27] Caution in interpreting small differences in coupling constants is therefore recommended, and even if they are meaningful, through-bond mechanisms must be considered. As is evident from the data presented in Table 5 and Figure 6, the extent of the observed $^{205}Tl-^{13}C$ coupling in **9** and **10** does not correlate simply with the distance of the carbon nuclei from the Tl(I) ion. For example, in **9** the average through-space distance from Tl to C7 (~4.0 Å) is similar to that to C11 (~4.1 Å) and slightly shorter than those to C12 and C13 (~4.6 Å), yet $^{205}Tl-^{13}C$ coupling is only observed in the ^{13}C NMR signals of the latter carbon atoms (C11–C13). The observation of ^{205}Tl coupling to some pyrazolyl ring carbons in some ligands but not in others, with no discernable trend (Figure 6), further attests to the difficulties associated with interpretation of structural features based on this NMR spectroscopic feature.

(26) Trofimenko, S.; Calabrese, J. C.; Kochi, J. K.; Wolowiec, S.; Hulsbergen, R. B.; Reedijk, J. *Inorg. Chem.* **1992**, *31*, 3943–3950.

(27) (a) Hinton, J. F.; Metz, K. R.; Briggs, R. W. In *Annual Reports on NMR Spectroscopy*; Webb, G. A., Ed.; Academic Press: New York, 1982; Vol. 13; pp 211–318. (b) Hinton, J. F.; Metz, K. R. In *NMR of Newly Accessible Nuclei*; Laszlo, P., Ed.; Academic Press: New York, 1983; Vol. 2; pp 367–384.

Table 5. ^1H and $^{13}C\{^1H\}$ NMR Data and Proposed Assignments for New Pyrazoles and Polypyrazole Ligands

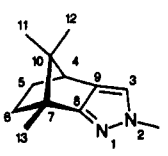
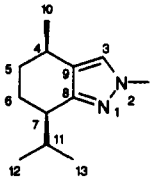
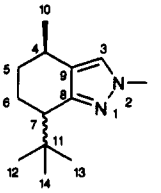

	^1H NMR		$^{13}C\{^1H\}$ NMR	
compd	signal (ppm)	assignmt	signal (ppm)	assignmt
cis-**2**[a]	0.85 (d, J = 7.0 Hz, 3H)	H12	18.7	C12
	1.05 (d, J = 7.0 Hz, 3H)	H13	21.1	C13
	1.21 (d, J = 7.0 Hz, 3H)	H10	21.7	C6
	1.49–1.56 (m, 1H)	H5a	22.6	C10
	1.66–1.72 (m, 1H)	H6a	26.6	C4
	1.76–1.85 (m, 2H)	H5b, H6b	30.3	C5
	2.14–2.22 (m, 1H)	H11	31.2	C11
	2.64–2.68 (m, 1H)	H7	39.2	C7
	2.78–2.84 (M, 1H)	H4	121.9	C3
	7.34 (s, 1H)	H3	133.5	C9
	12.2 (br s, 1H)	H2	144.4	C8
cis-**3**[a]	1.04 (s, 9H)	H12, H13, H14	22.4	C10
	1.19 (d, 3H, J = 6.5 Hz)	H10	23.3	C6
	1.54–1.60 (m, 1H)	H5a	26.4	C4
	1.72–1.78 (m, 2H)	H5b, H6a	29.0	C12, C13, C14
	1.84–1.91 (m, 1H)	H6b	30.6	C5
	2.55–2.60 (m, 1H)	H7	34.5	C11
	2.75–2.82 (m, 1H)	H4	43.3	C7
	7.35 (s, 1H)	H3	123.3	C3
	9.44 (s, 1H)	H2	133.2	C9
			143.3	C8
trans-**3**[a]	1.04 (s, 9H)	H12, H13, H14	21.4	C10
	1.08–1.14 (m, 1H)	H5a	26.4	C6
	1.20 (d, J = 7.0 Hz, 3H)	H10	28.3	C12, C13, C14
	1.46–1.55 (m, 1H)	H6a	28.4	C4
	1.90–1.94 (m, 1H)	H5b	33.3	C5
	2.00–2.02 (m, 1H)	H6b	34.4	C11
	2.58–2.64 (m, 2H)	H4, H7	44.5	C7
	7.35 (s, 1H)	H3	124.1	C3
	9.30 (br s, 1H)	H2	131.7	C9
			144.2	C8
6[b]	0.62 (s, 3 H)	H12	10.3	C13
	0.94 (s, 3H)	H11	18.7	C11
	1.20–1.26 (m, 4 H)	H13, H5a	20.4	C12
	1.36–1.41 (m, 1 H)	H6a	26.8	C5
	1.81–1.87 (m, 1 H)	H6b	32.9	C6
	2.04–2.10 (m, 1 H)	H5b	46.4	C4
	2.76 (d, J = 4.0 Hz, 1 H)	H4	50.3	C10
	7.22 (s, 1 H)	H3	59.9	C3
			125.7 (d, J_{CP} = 10.9 Hz)	C3
			130.2 (d, J_{CP} = 9.2 Hz)	C9
			174.4 (d, J_{CP} = 14.7 Hz)	C8
7[a]	0.84 (d, J = 6.8 Hz, 9H)	H12	19.0	C12
	0.97 (d, J = 6.9 Hz, 9H)	H13	20.8	C13
	1.17 (d, J = 6.9 Hz, 9H)	H10	21.8	C6
	1.37–1.56 (m, 3H)	H5a	22.2	C10
	1.60–1.82 (m, 9H)	H6a, H6b, H5b	26.8	C4
	2.12–2.21 (m, 3H)	H11	29.6	C5
	2.57–2.65 (m, 3H)	H7	31.0	C11
	2.73–2.82 (m, 3H)	H4	40.5	C7
	7.51 (s, 3H)	H3	127.2 (d, J_{CP} = 7.2 Hz)	C3
			132.1 (d, J_{CP} = 12.0 Hz)	C9
			160.6 (d, J_{CP} = 14.5 Hz)	C8
8[a]	0.96 (s, 27H)	H12, H13, H14	20.8	C10
	1.15 (m, 12H)	H10, H5a	25.8	C6
	1.35–1.48 (m, 3H)	H6a	27.9	C12, C13, C14
	1.82–1.89 (m, 3H)	H5b	28.4	C4
	1.98–2.02 (m, 3H)	H6b	32.7	C5
	2.51–2.56 (m, 6H)	H4, H7	34.2	C11
	7.56 (s, 3H)	H3	44.8	C7
			128.6 (d, J_{CP} = 7.3 Hz)	C9
			130.7 (d, J_{CP} = 12.2 Hz)	C3
			159.3 (d, J_{CP} = 14.6 Hz)	C8

Table 5. (Continued)

compd	^{1}H NMR signal (ppm)	^{1}H NMR assignmt	^{13}C{^{1}H} NMR signal (ppm)	^{13}C{^{1}H} NMR assignmt
9[a]	0.98 (d, J = 7.3 Hz, 9H)	H12	19.2	C12
	1.18 (d, J = 6.1 Hz, 9H)	H13	22.3 (d, J_{CTl} = 119.9 Hz)	C13
	1.29 (d, J = 7.3 Hz, 9H)	H10	23.0	C10
	1.51–1.60 (m, 3H)	H5a	23.3	C6
	1.72–1.79 (m, 3H)	H6a	27.4	C4
	1.82–1.88 (m, 3H)	H5b	29.9	C5
	1.96–2.14 (m, 3H)	H6b	32.2 (d, J_{CTl} = 148.6 Hz)	C11
	2.24–2.44 (br m, 3H)	H11	40.2	C7
	2.69–2.76 (m, 3H)	H7	121.5	C9
	2.84–2.90 (m, 3H)	H4	133.3	C3
	7.58 (s, 3H)	H3	153.0	C8
10[c]	0.87 (s, 27H)	H12, H13, H14	21.2	C10
	0.98–1.04 (m, 3H)	H5a	26.1	C6
	1.06 (d, J = 7.4 Hz, 9H)	H10	27.7 (d, J_{CTl} = 80 Hz)	C12, C13, C14
	1.38–1.46 (m, 3H)	H6a	28.4	C4
	1.66–1.74 (m, 3H)	H5b	33.5	C5
	1.82–1.88 (m, 3H)	H6b	34.6	C11
	2.42–2.48 (m, 3H)	H4	43.1	C7
	2.50–2.56 (m, 3H)	H7	125.3	C9
	7.49 (s, 3H)	H3	131.2	C3
			150.5	C8

[a] ^{1}H and ^{13}C{^{1}H} NMR spectra recorded in CD_2Cl_2 at 500 and 125 MHz, respectively. [b] In $CDCl_3$. [c] In benzene-d_6.

Conclusion

Reproducible and large-scale syntheses of novel optically active and C_3-symmetric tris(pyrazolyl)hydroborate and tris(pyrazolyl)phosphine oxide ligands well-suited for the construction of metal complexes that may mediate stereoselective transformations have been developed. The new ligands have been characterized in solution by NMR spectroscopy and in the solid state by X-ray crystallography. The disposition of sterically encumbered groups on the stereogenic centers of the pyrazolyl moieties is anticipated to result in unique asymmetric cavities about coordinated metal ions,[7] the structures of the Tl(I) species **9** and **10** being indicative of the steric properties and rotational symmetry to be expected. With the synthesis of the new ligands described herein, the growing class of enantiomerically enriched multidentate chelates with high ($>C_2$) rotational symmetry[3,28] has been augmented and unique opportunities to assess the possible repercussions of such geometric features on enantioselective processes have become available.

Experimental Section

Materials and Methods. All solvents and reagents are commercially available and were used as received, except benzene and THF, which were distilled from sodium benzophenone ketyl. NMR spectra were recorded on Bruker AC-200, AC-300, Varian VXR-300, or VXR-500 NMR spectrometers. ^{1}H and ^{13}C{^{1}H} NMR chemical shifts are reported versus tetramethylsilane and referenced to the residual solvent peak(s); data for the pyrazoles and ligands derived therefrom are listed in Table 5. ^{31}P{^{1}H} NMR chemical shifts are reported versus external H_3PO_4 (85%). FTIR spectra were recorded on a Perkin-Elmer Model 1600 FT-IR spectrometer and mass spectra were determined using a Finnigan 4000 mass spectrometer with 70-eV electron impact ionization. Optical rotations were measured and error analysis performed according to a literature procedure[29] using a 5-cm cell and a Perkin-Elmer 241 polarimeter. Elemental analyses were performed by Atlantic Microlabs, Inc.

(4*S*,7*R*)-7,8,8-Trimethyl-4,5,6,7-tetrahydro-4,7-methano-2-indazole (1). To a slurry of KH (30.1 g, 0.330 mol, 35% oil suspension washed with hexanes) in THF (70 mL) was added (*R*)-(+)-camphor (10.1 g, 0.0661 mol). Gas evolution commenced immediately. The mixture was refluxed for 15 min until gas evolution ceased and was then cooled to room temperature. Ethyl formate (22 mL, 0.27 mol) was added dropwise over 2 h, and the mixture was then stirred for an additional 16 h. After quenching (5 mL of 2-propanol and 150 mL of H_2O), the mixture was treated with Et_2O (3 × 50 mL) and then acidified to pH 1 with concentrated HCl. An oil separated which was extracted with Et_2O, the extracts were dried with $MgSO_4$, and solvent was removed under reduced pressure to afford 3-(hydroxymethylene)-1,7,7-trimethylbicyclo[2.2.1]hexan-2-one as a pale tan solid, identified by comparison of NMR and IR spectra with previously published data (11.1 g, 92%).[8a,18]

A solution of the above solid (8.67 g, 0.0482 mol) and hydrazine monohydrate (2.43 mL, 0.0491 mol) in MeOH (500 mL) was refluxed for 17 h. Solvent was removed under reduced pressure, and the resulting yellow solid was recrystallized from acetone to yield **1** as pale yellow blocks (7.68 g, 90%). Analytical and spectroscopic data for **1** matched those published previously.[8a]

7(*R*)-Isopropyl-4(*R*)-methyl-4,5,6,7-tetrahydro-2*H*-indazole [*cis*-2]. (2*S*,5*R*)-Menthone (95%) (150 g, 0.97 mol) was formylated according to a literature procedure,[30] except the reaction was stirred for 16 h and the crude product was purified by chromatography (silica, 25:1 hexane–acetone as eluent), followed by distillation at 80–90 °C under vacuum (~0.3 Torr). The resulting colorless oil was comprised of a 13:1 ratio of (3*R*,6*R*)- and (3*R*,6*S*)-2-(hydroxymethylene)-6-isopropyl-3-methylcyclohexanones [(3*R*,6*R*)- and (3*R*,6*S*)-**5**] according to ^{1}H and

(28) (a) Halterman, R. L.; Jan, S.-T. *J. Org. Chem.* **1991**, *56*, 5253–5254. (b) Proess, G.; Hevesi, L. *J. Mol. Catal.* **1993**, *80*, 395–401.

(29) Dewey, M. A.; Gladysz, J. A. *Organometallics* **1993**, *12*, 2390–2397.

(30) Potapov, V. M.; Kiryushkina, G. V.; Talebarovskaya, I. K.; Shapet'ko, N. N.; Radushnova, I. L. *Zh. Org. Khim.* **1973**, *9*, 2134–2140.

$^{13}C\{^1H\}$ NMR spectroscopy. The mixture (103 g, 0.57 mol) was refluxed with hydrazine monohydrate (30.2 mL, 0.62 mol) in MeOH (500 mL) for 1 h. Solvent was removed under reduced pressure, and the remaining green oil was dissolved in CH_2Cl_2 (150 mL) and subjected to an aqueous workup. The oil resulting after solvent removal from the organic fraction [96 g, 0.54 mol of a 13:1 mixture of *cis*- and *trans*-**2** by ^1H and $^{13}C\{^1H\}$ NMR spectroscopy] was dissolved in CH_2Cl_2 (250 mL). This solution was treated with concentrated HCl (250 mL) at room temperature, and after rapid stirring for 10 min, the organic layer was separated and the aqueous layer was extracted with 3 × 100 mL of CH_2Cl_2. The combined organic extracts were dried with $MgSO_4$ and concentrated to afford a light tan solid (114.5 g, 0.54 mol). The solid was triturated with anhydrous Et_2O, dried, and then recrystallized from $CHCl_3$/*tert*-butyl methyl ether to afford 15.0 g of a 1.5:1 mixture of the hydrochloride salts of *cis*- and *trans*-**2** (^1H NMR). Pure *cis*-**2**·HCl was obtained by further $CHCl_3$/*tert*-butyl methyl ether recrystallizations of the residue remaining upon removal of solvent from the mother liquor (51.0 g, 32% yield): mp 175–178 °C; $[\alpha]_D^{22} = +86 \pm 1°$ (*c* 1.2 × 10^{-3} g/mL, $CHCl_3$); ^1H NMR ($CDCl_3$, 300 MHz) δ 7.63 (s, 1H), 2.83 (m, 2H), 2.49 (m, 1H), 1.68 (m, 4H), 1.20 (d, J = 5.9 Hz, 3H), 1.08 (d, J = 6.8 Hz, 3H), 0.83 (d, J = 6.8 Hz, 3H) ppm; $^{13}C\{^1H\}$ NMR ($CDCl_3$, 75 MHz) δ 146.7, 129.1, 123.6, 37.8, 30.3, 28.7, 25.4, 21.7, 20.7, 19.6, 17.8 ppm; IR (KBr) 2957, 1551, 1467, 1367, 1202, 1173, 1090, 918 cm^{-1}. Anal. Calcd for $C_{11}H_{19}N_2Cl$: C, 61.52; H, 8.92; N, 13.05. Found: C, 61.60; H, 8.94; N, 13.21.

A solution of *cis*-**2**·HCl (47 g, 0.22 mol) in CH_2Cl_2 (400 mL) was added to a solution of $NaHCO_3$ (51 g, 0.61 mol) in H_2O (500 mL), and the mixture was stirred for 10 min. The organic and aqueous layers were separated, and the aqueous layer was extracted with CH_2Cl_2 (3 × 100 mL). The organic layers were combined and dried with Na_2CO_3, and the solvent was removed under reduced pressure to afford *cis*-**2** as a viscous pale yellow oil which solidified after 24 h (35 g, >97% pure by ^1H NMR, 90% yield): mp 55–56 °C; $[\alpha]_D^{24} = 39.5 \pm 0.2°$ (*c* 5.2 × 10^{-3} g/mL, $CHCl_3$); IR (KBr) 3192, 2952, 2865, 1562, 1493, 1468, 1376, 1296, 1145, 1056, 950 cm^{-1}; MS (rel intensity) 178 (M^+, 15), 135 (100). Anal. Calcd for $C_{11}H_{18}N_2$: C, 74.11; H, 10.18; N, 15.71. Found: C, 74.00; H, 10.24; N, 15.71.

2-(Hydroxymethylene)-6-*tert*-butyl-3-methylcyclohexanone. The following modified version of a previously reported procedure[19] for the synthesis of 2-*tert*-butyl-5(*R*)-methylcyclohexanone facilitates isolation of the product on a large scale. To a mechanically stirred solution of MeMgBr (1300 mL, 2.4 mol, 1.85 M solution in Et_2O) at 0 °C was added CuI (18.5 g, 0.097 mol). The mixture was stirred at 0 °C for 0.75 h, and then (*R*)-(+)-pulegone (225 mL, 1.40 mol) in Et_2O (600 mL) was added dropwise over a 6-h period. Following the addition the reaction mixture was stirred at 0 °C for 2 h, warmed to room temperature, and stirred for an additional 13 h. The mixture was then recooled to 0 °C and treated with H_2O (270 mL) followed by a solution of NH_4Cl (55 g) in H_2O (500 mL) and then concentrated HCl (175 mL). The organic layer was separated, and the aqueous layer was extracted with Et_2O (3 × 200 mL). The combined organic layers were washed with saturated aqueous $NaHCO_3$ (500 mL), dried with $MgSO_4$, and concentrated to a yellow-brown oil which was distilled under vacuum (40–45 °C, 5 Torr) to yield 2-*tert*-butyl-5(*R*)-methylcyclohexanone as a colorless oil (238 g, ~80% pure by ^1H NMR vs ferrocene standard, used for the next reaction without further purification).

To a mechanically stirred suspension of NaOMe (159 g, 3.00 mol) in toluene (1500 mL) at room temperature was added ethyl formate (238 mL, 3.00 mol) in toluene (250 mL) followed by 2-*tert*-butyl-5(*R*)-methylcyclohexanone (236 g, ~80% pure, ~1.1 mol) in toluene (250 mL). The mixture was stirred for 14 h and then quenched with H_2O (800 mL). The aqueous layer was separated, and the organic layer was extracted with 20% aqueous NaOH (3 × 200 mL). The combined aqueous layers were washed with hexane (200 mL) and then acidified with concentrated HCl to a pH of 1. The oil which separated was extracted with Et_2O (3 × 200 mL). The combined organic layers were dried with $MgSO_4$, concentrated to a brown oil, which was passed through a silica gel pad (hexane/acetone 25:1 as the eluent), and then distilled under vacuum (58–60 °C, 5 Torr) to yield 2-(hydroxymethylene)-6-*tert*-butyl-3-methylcyclohexanone as a ~2:1 mixture of diastereomers in both keto and enol forms that was of sufficient purity to be used for the synthesis of **3** (115 g, 42% from (*R*)-(+)-pulegone): ^1H NMR ($CDCl_3$, 300 MHz) δ 13.74 (d, J = 3.4 Hz, 2H), 13.13 (d, J = 5.2 Hz, 1H), 8.52 (d, J = 3.3 Hz, 2H), 8.31 (d, J = 5.9 Hz, 1H), 1.84 (m, 36H), 0.96 (m, 72H) ppm; $^{13}C\{^1H\}$ NMR ($CDCl_3$, 75 MHz) δ 189.0, 187.0, 181.4, 181.1, 116.1, 115.7, 71.3, 69.9, 59.9, 59.0, 51.4, 49.9, 36.6, 34.8, 34.1, 33.7, 31.9, 30.2, 29.4, 29.1, 29.0, 28.7, 27.9, 27.7, 27.7, 27.6, 27.4, 24.8, 24.3, 24.2, 24.1, 22.2, 21.1, 20.9, 20.1, 19.9 ppm; IR (thin film) 2958, 2870, 1732, 1703, 1592, 1480, 1456, 1394, 1366, 1308, 1220, 1199, 1089, 922 cm^{-1}; high-resolution MS (EI) calcd for $C_{12}H_{20}O_2$ (M) *m/e* 196.1463, found 196.1451.

7(*R*)-*tert*-Butyl-4(*R*)-methyl-4,5,6,7-tetrahydro-2*H*-indazole and 7(*S*)-*tert*-Butyl-4(*R*)-methyl-4,5,6,7-tetrahydro-2*H*-indazole [*cis*-3 and *trans*-3]. To a stirred solution of 2-(hydroxymethylene)-6-*tert*-butyl-3-methylcyclohexanone (114 g, 0.58 mol) in MeOH (400 mL) was added hydrazine monohydrate (31.0 mL, 0.638 mol), and the mixture was stirred for 1.5 h at room temperature. Solvent was removed under reduced pressure, and the residue was dissolved in CH_2Cl_2 (300 mL), washed with H_2O (300 mL), dried with Na_2CO_3, and concentrated to a viscous green oil which solidified upon full drying under high vacuum (~2:1 ratio of *cis*- and *trans*-**3**). Recrystallization from heptane at −20 °C yielded a first crop of the minor isomer *trans*-**3** as a yellow microcrystalline solid (31.5 g, >95% pure by ^1H NMR).

The mother liquor, further enriched in *cis*-**3** (~3:1 ratio of diastereomers), was concentrated and dissolved in CH_2Cl_2 (250 mL). This solution was treated with concentrated HCl (250 mL) at room temperature, and after rapid stirring for 10 min, the organic layer was separated and the aqueous layer was extracted with CH_2Cl_2 (3 × 100 mL). The combined organic extracts were dried with Na_2SO_4 and concentrated to a light tan solid. The solid was triturated with Et_2O, dried, and recrystallized several times from toluene until the mother liquor was composed entirely of *cis*-**3**·HCl (>95% pure by ^1H NMR, 17.8 g, 13% total yield from 2-(hydroxymethylene)-6-*tert*-butyl-3-methylcyclohexanone): mp 153–155 °C; $[\alpha]_D^{22} = +46.4 \pm 0.4°$ (*c* 2.1 × 10^{-3} g/mL, $CHCl_3$); ^1H NMR ($CDCl_3$, 300 MHz) δ 7.77 (s, 1H), 2.68 (m, 2H), 1.95 (m, 1H), 1.70 (m, 2H), 1.51 (m, 1H), 1.14 (d, J = 6.8 Hz, 3H), 0.97 (s, 9H) ppm; $^{13}C\{^1H\}$ NMR ($CDCl_3$, 75 MHz) δ 144.9, 129.9, 124.8, 41.5, 34.3, 29.0, 28.7, 25.8, 23.0, 21.3 ppm; IR (KBr) 2955, 1718,

1685, 1654, 1542, 1458, 1368, 1203, 1182, 1098, 926 cm^{-1}. Anal. Calcd for $C_{12}H_{21}N_2Cl$: C, 63.00; H, 9.25; N, 12.25. Found: C, 62.81; H, 9.24; N, 12.38.

The precipitates from the toluene recrystallizations, which were composed of *cis*-**3**·HCl and *trans*-**3**·HCl in a 1:1 ratio, were combined, treated with $NaHCO_3$ in H_2O/CH_2Cl_2, subjected to an aqueous workup, and recrystallized from heptane to obtain an additional 10.0 g of the minor isomer *trans*-**3** (>95% pure by ^{1}H NMR, 41.5 g, 37% total yield from 2-(hydroxymethylene)-6-*tert*-butyl-3-methylcyclohexanone): mp 137–139 °C; $[\alpha]_D^{22} = -83.5 \pm 0.4°$ (*c* 2.3 × 10^{-3} g/mL, $CHCl_3$); IR (KBr) 3228, 2951, 2865, 1560, 1464, 1361, 1280, 1140, 1062, 944 cm^{-1}; high-resolution MS (EI) calcd for $C_{12}H_{20}N_2$ (M) *m/e* 192.1626, found 192.1625. Anal. Calcd for $C_{12}H_{20}N_2$: C, 74.95; H, 10.48; N, 14.57. Found: C, 74.87; H, 10.47; N, 14.50.

Compound *cis*-**3**·HCl was treated with $NaHCO_3$ in an identical manner to obtain pure *cis*-**3** as a light yellow viscous oil (>95% pure by ^{1}H NMR, 14.4 g, 96% yield from the salt): $[\alpha]_D^{22} = +21.4 \pm 0.3°$ (*c* 1.1 × 10^{-3} g/mL, $CHCl_3$); IR (thin film) 3194, 2954, 1504, 1480, 1454, 1365, 1202, 1101, 1060, 957 cm^{-1}; high-resolution MS (EI) calcd for $C_{12}H_{20}N_2$ (M) *m/e* 192.1626, found 192.1617.

Tris[(4*S*,7*R*)-7,8,8-trimethyl-4,5,6,7-tetrahydro-4,7-methano-2-indazolyl]phosphine Oxide (6). To a stirred solution of (4*S*,7*R*)-7,8,8-trimethyl-4,5,6,7-tetrahydro-4,7-methano-2-indazole (2.01 g, 0.0119 mol) and triethylamine (1.57 g, 0.0156 mol) in dry benzene (20 mL) at 0 °C was added $POCl_3$ (0.583 g, 0.0380 mol) dropwise over 0.5 h. The mixture was then refluxed for 20 h. Filtration followed by removal of solvent from the filtrate under reduced pressure yielded a tan residue which was recrystallized from CH_2Cl_2/toluene (1:1) to afford colorless **6** (1.44 g, 60%): mp 220 °C dec; $[\alpha]_D^{23} = +4.0 \pm 0.2°$ (*c* 5.2 × 10^{-3} g/mL, $CHCl_3$); $^{31}P\{^1H\}$ NMR ($CDCl_3$, 121 MHz) δ −14.5 (s) ppm; IR (KBr) 2962, 1609, 1336, 1296, 1256, 1207, 1175, 1083, 911 cm^{-1}; MS (rel intensity) 572 (M^+, 20), 133 (100). Anal. Calcd for $C_{33}H_{45}N_6OP$: C, 69.21; H, 7.92; N, 14.67. Found: C, 68.63; H, 7.88; N, 14.81.

Tris[7(*R*)-isopropyl-4(*R*)-methyl-4,5,6,7-tetrahydro-2-indazolyl]phosphine Oxide (7). The synthesis was performed as described above for the synthesis of **6**, except the product was crystallized from Et_2O at −30 °C to yield **7** as white needles. After the product was washed with cold Et_2O and the filtrate cooled a second crop of crystals was collected (1.34 g, 62% yield overall): mp 137–138 °C; $[\alpha]_D^{23} = +41.2 \pm 0.2°$ (*c* 6.1 × 10^{-3} g/mL, CH_2Cl_2); $^{31}P\{^1H\}$ NMR ($CDCl_3$, 121 MHz) δ −12.4 (s) ppm; IR (KBr) 2956, 2870, 1578, 1560, 1543, 1508, 1333, 1302, 1286, 1108, 1090, 962, 807, 722, 621, 554 cm^{-1}. Anal. Calcd for $C_{33}H_{51}N_6OP$: C, 68.48; H, 8.88; N, 14.52. Found: C, 67.14; H, 8.96; N, 14.39. The results of carbon analyses have consistently been lower than predicted despite clear evidence of high purity from ^{1}H and ^{13}C NMR spectra and a sharp melting point.

Tris[7(*S*)-*tert*-butyl-4(*R*)-methyl-4,5,6,7-tetrahydro-2-indazolyl]phosphine Oxide (8). The synthesis was performed on a 1.50-g scale as described above for the synthesis of **6** and **7**, except the product was crystallized from heptane at −20 °C (0.960 g, 60%): mp 135–137 °C; $[\alpha]_D^{22} = -195 \pm 2°$ (*c* 1.1 × 10^{-3} g/mL, toluene); $^{31}P\{^1H\}$ NMR ($CDCl_3$, 121 MHz) δ −8.16 ppm; IR (KBr) 2958, 2867, 1578, 1480, 1456, 1314, 1283, 1100, 1086, 962 cm^{-1}. Anal. Calcd for $C_{36}H_{57}N_6OP$: C, 69.64; H, 9.25; N, 13.54. Found: C, 68.40; H, 9.23; N, 13.42.

Thallium Tris[7(*R*)-isopropyl-4(*R*)-methyl-4,5,6,7-tetrahydro-2-indazolyl]hydroborate ($TlTp^{Menth}$, 9). Pyrazole *cis*-**2** (10.0 g, 0.0561 mol) and KBH_4 (1.10 g, 0.0204 mol) were gradually heated to 210 °C with monitoring of H_2 evolution using a wet-test meter. Heating was continued at that temperature until gas evolution ceased (~5 h, ~1 equiv of H_2 evolved). The mixture was then allowed to cool under an atmosphere of dinitrogen, and the resulting glassy solid was extracted with CH_2Cl_2 (150 mL) and filtered through a Celite pad. To the filtrate was added TlOAc (6.59 g, 0.025 mol), and the mixture was stirred for 3 h and then filtered. Removal of the solvent from the filtrate under reduced pressure yielded a white solid, which after washing with cold MeOH and vacuum drying was identified as pure **9** (14 g, 74% yield). Recrystallization from toluene/MeOH yielded crystals suitable for X-ray crystallography: mp 178–179 °C; $[\alpha]_D^{24} = +210 \pm 2°$ (*c* 1.7 × 10^{-3} g/mL, $CHCl_3$); IR (KBr) 2955, 2866, 2430 (BH), 1553, 1451, 1390, 1309, 1144, 1014, 826, 776, 737, 715, 696 cm^{-1}. Anal. Calcd for $C_{33}H_{52}N_6BTl$: C, 52.99; H, 7.01; N, 11.24. Found: C, 53.19; H, 7.15; N, 11.43.

Thallium Tris[7(*S*)-*tert*-butyl-4(*R*)-methyl-4,5,6,7-tetrahydro-2-indazolyl]hydroborate ($TlTp^{Mementh}$, 10). A procedure analogous to that used to prepare **9** was used, except with *trans*-**3** (5.10 g, 0.0265 mol) as starting material and a thermolysis temperature of 240 °C (yield 4.3 g, 62%): mp 193–195 °C; $[\alpha]_D^{22} = -593 \pm 9°$ (*c* 9.7 × 10^{-4} g/mL, toluene); IR (KBr) 2951, 2866, 2427 (BH), 1554, 1478, 1467, 1456, 1362, 1242, 1141, 1014, 941 cm^{-1}. Anal. Calcd for $C_{36}H_{58}N_6BTl$: C, 54.73; H, 7.40; N, 10.64. Found: C, 55.00; H, 7.40; N, 10.96.

X-ray Crystallography. Colorless crystals of dimensions 0.60 × 0.45 × 0.1 mm (**6**), 0.60 × 0.45 × 0.35 mm (**9**), or 0.49 × 0.34 × 0.25 mm (**10**) were mounted on a glass fiber with epoxy and placed on an Enraf-Nonius CAD-4 diffractometer with graphite-monochromated Mo Kα (λ = 0.710 73 Å) radiation. Important crystallographic information is summarized in Table 1. Cell constants were obtained from a least-squares refinement of the setting angles of 23, 47, or 25 carefully centered reflections in the range 22.00° < 2θ < 44.00°, 22.00° < 2θ < 42.00°, or 29.00° < 2θ < 39.90°, respectively, for **6**, **9**, and **10**. The intensity data were collected using the ω-2θ scan technique to the maximum 2θ values noted in Table 1. Empirical absorption corrections were applied using either the program DIFABS[31] (**6** and **9**) or azimuthal scans of several reflections (**10**) which resulted in transmission factors ranging from 0.79 to 1.28, 0.89 to 1.12, or 0.77 to 1.00, respectively. The data were corrected for Lorentz and polarization effects, but no decay corrections were needed.

The structures were solved by direct methods[32] using the TEXSAN[33] software package. Non-hydrogen atoms were refined anisotropically, and the H atoms were placed at calculated positions. The maximum and minimum peaks on the final difference Fourier maps corresponded to 0.33 and −0.30 e$^-$/Å^3 for **6**, 0.87 and −0.82 e$^-$/Å^3 for **9**, and 1.15 and −1.15 e$^-$/Å^3 for **10**. Neutral atom scattering factors and anomalous dispersion terms were taken from the literature.[34,35] For **6**, the absolute configuration of the

(31) Walker, N.; Stuart, D. *Acta Crystallogr.* **1983**, *A39*, 158–166.
(32) Calabrese, J. C. PHASE: Patterson Heavy Atom Solution Extractor. Ph.D Thesis, University of Wisconsin, Madison, WI, 1972.
(33) *TEXSAN-Texray Structure Analysis Package*, Molecular Structure Corp., 1985.

camphor rings was chosen to match that of the (*R*)-(+)-camphor starting material. The enantiomeric forms of the pyrazolyl rings in **9** and **10** were chosen by assuming that the absolute configuration at the 4-position of the 6-membered ring (containing the methyl group) remained unchanged throughout the ligand synthesis. This assumption was checked in the case of **9** by carrying out refinement of the X-ray data (including Friedel pairs) with the opposite enantiomer; convergence was reached with significantly higher values for *R* (0.058), R_w (0.061), and goodness of fit (1.96 versus 1.22). Drawings of the structures appear in Figures 1–5, with selected bond lengths and angles listed in the figure captions. Selected final atomic positional parameters and *B*(eq) values (excluding H atoms) are listed in Tables 2–4. Completely labeled ORTEP drawings and full tables of bond lengths and angles, atomic positional parameters, and final thermal parameters for non-hydrogen atoms are given for **9** and **10** in the supplementary material (Figure S1 and Tables S1–S8) and for **6** in the supplementary material of its preliminary communication.[6a]

Acknowledgment. We thank Professor Doyle Britton for his work on the X-ray crystal structures, Professor Gerard Parkin (Columbia University) for providing access to unpublished results, and Professor Jose Elguero (Instituto de Quimica Medica, Madrid) for bringing his work to our attention. Financial support was provided by the Petroleum Research Fund, administered by the American Chemical Society, the National Science Foundation (CHE-9207152 and a National Young Investigator Award), the University of Minnesota's Undergraduate Research Opportunities Program (D.D.L), and the University of Minnesota.

Supplementary Material Available: Fully labeled ORTEP drawings and tables of fractional coordinates, bond distances and angles, and anisotropic thermal parameters for the X-ray structures of $TlTp^{Menth}$ (**9**) and $TlTp^{Mementh}$ (**10**) and representative 2D NMR spectroscopic data (28 pages). Ordering information is given on any current masthead page.

OM940046Z

(34) Cromer, D. T. *International Tables for X-ray Crystallography*; The Kynoch Press: Birmingham, United Kingdom, 1974; Vol. IV, Tables 2.2A and 2.3.1.

(35) Ibers, J. A.; Hamilton, W. C. *Acta Crystallogr.* **1964**, *17*, 781.